

Zemax Module 2

CHRIS MAY¹

¹Master's Industrial Internship Program, University of Oregon, 1252 University of Oregon, Eugene, OR, 97403

*Corresponding author: cmay7@uoregon.edu

Compiled July 30, 2018

In this module, OpticStudio is used to design a Polygon Scanner with the assistance of a simple macro-solve. A Gaussian source is coupled into a single mode optical fiber using only components from the Thorlabs catalog using the single mode coupling function and physical optics. And an optic is designed for viewing samples in an optical cryostat.

<http://dx.doi.org/10.1364/ao.XX.XXXXXX>

1. THE POLYGON SCANNER

The goal of this section of the lab is to design a polygon scanner for a 5mm HeNe laser beam. The device needs to scan through 10° through a $F/3$ lens and have the smallest RMS spot size possible.

A. Background

A general polygon scanner consists of a reflective material which is cut into the shape of a polygon, typically a hexagon or octagon, and then rotated about its axis. A beam is pulsed and reflected off the device as it spins and causes the laser to scan across a material [1]. If the beam is powerful enough it can be used to micro-machine textures into the surface of the imaging plane, and with the assistance of a demagnifying lens the beam can be focused down to a very small spot size for high precision texturing. There are applications for this type of device in semiconductor fabrication [2] as well as Optical Coherence Tomography [3].

B. Methods

A 633nm HeNe source was propagated through a 3mm aperture. A mirror was placed 10mm from the aperture at a 45° angle with respect to the y-axis. To mimic the polygon scanner, the mirror was increased to a thickness of 10mm and then rotated by 5°. The rotation was applied to the front surface as shown in Fig. 1 which is the incorrect axis of rotation for a

polygon scanner so a macro was written to decenter the entire mirror based off the angle of rotation.

The macro solve shown in Fig. 2 found the angle from the mirror's coordinate break surface properties and then shifted the entire surface accordingly to treat the back axis as the center of the polygon scanner which is shown in Fig. 4. The macro was written in the Zemax Programming Language (ZPL) under the programming tab. The first task was to find the surface properties from the lens data editor which is performed by the SPRX command [4]. Specific parameter codes and parameter numbers which were required to find the angle of rotation of that surface can be determined with the OpticStudio "Help System". Once the angle is known, it needs to be translated into radians, as ZPL only has radian based trigonometric functions. But there is no π term in ZPL, so it must be solved for with an arc-trigonometric function, in this case an arc-cosine was used. The SOLVERRETURN function was finally used to decenter the mirror by $d \sin(\theta)$ and the translation was finished.

Once the object was manipulated to shift as a function of the angle of rotation, a lens was added to the system and the multiconfiguration editor was used to incorporate multiple rotations into the optimization. The thickness and radius of the first half of the doublet were set to be variable, as well as the thickness of the rear half of the doublet.

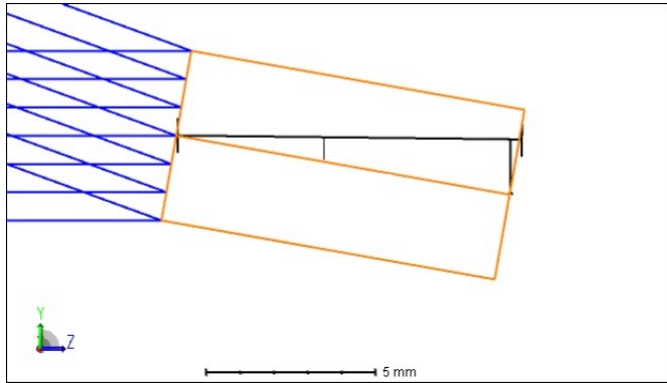


Fig. 1. Mirror rotation about front face

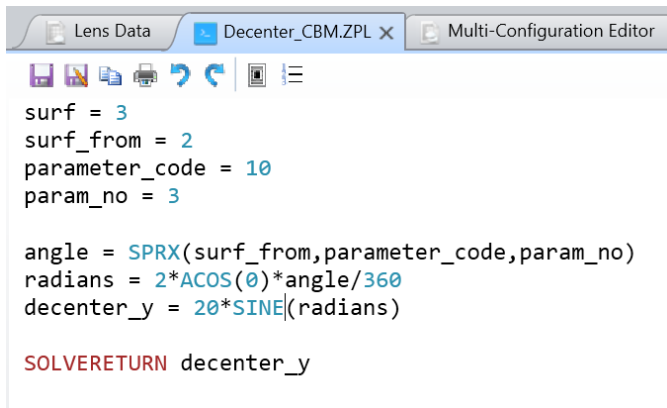


Fig. 2. Macro solve for decentering mirror.

For the optimization, Gaussian Quadrature was used for 8 arms and 4 rings. The criterion for optimization was the RMS Spot size with the centroid as the reference. The boundary values for glass were minimum 0.5mm to maximum 10mm with an edge thickness of 0.5mm. For air, the boundary values were a minimum of 0.5mm to a maximum of 1m and edge thickness 0.5mm. Axial symmetry can't be assumed for this system due to the rotations. The end merit function came out to be 0.1358 for all three configurations.

C. Results

The beam reflects off the surface and propagates through a $F/3$ lens 5mm from the scanner onto the imaging plane. On the imaging plane the beam is about 1.7mm from the central axis and has an RMS spot size radius of $19\mu\text{m}$ at a reflection angle $\theta = 0^\circ$ (Fig. 6) and $22\mu\text{m}$ for the $\theta = \pm 5^\circ$ angles (Fig. 7). This isn't an extremely small spot size, but it is one of the setups which had the smallest difference between spot size at 0° and $\pm 5^\circ$. If the device is being used to machine some material it would be desirable for the

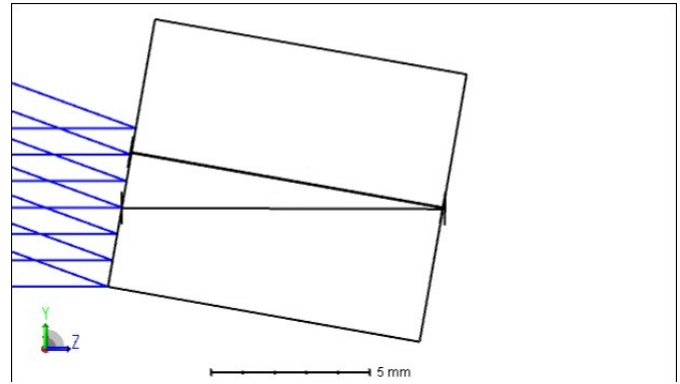


Fig. 3. Mirror rotation about rear face or center of polygon scanner

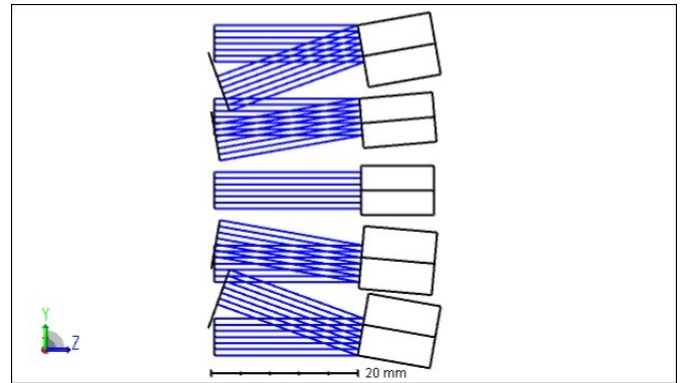


Fig. 4. Scanning through $\pm 10^\circ$ about the rear axis of rotation with the decentering macro

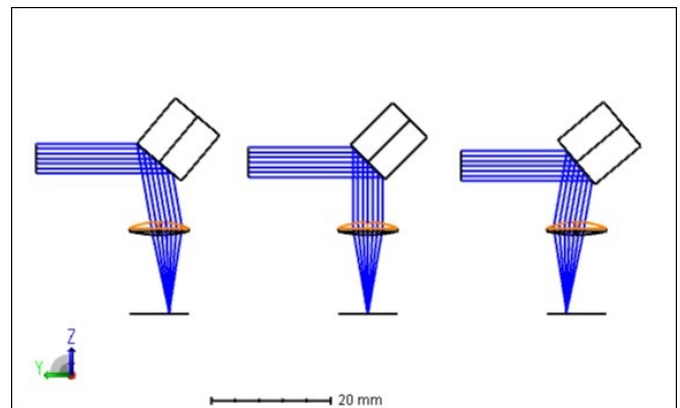


Fig. 5. Model polygon scanner, scanning across $\pm 5^\circ$ through a lens

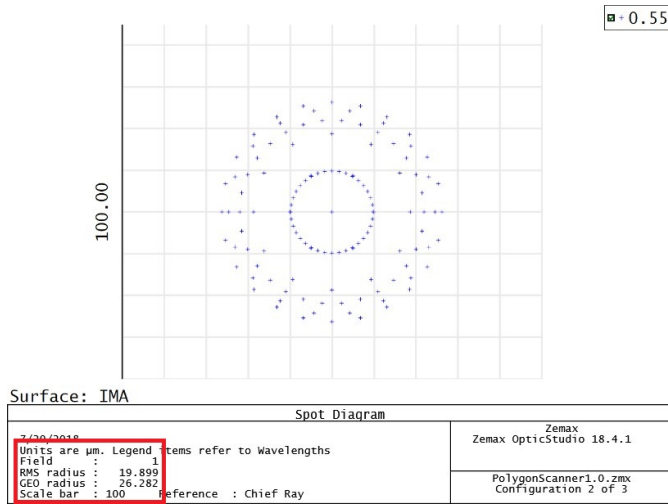


Fig. 6. Incident spot size on imaging plane.

beam to be about the same size throughout the entire scan. A variety of different types of glasses were tested within the Schott and Nikon libraries, and the glasses which seemed to minimize the radius of the beam were N-SF66 for the front and N-FK58 for the rear of the doublet [5].

A device of these specifications could be produced in a laboratory setting or even as a compact product for manufacturing. The overall size is a few centimeters and the beam size would be suitable for laser etching of metals.

2. FIBER COUPLING

The goal is to couple a 3mm HeNe beam into a single mode optical fiber with only materials from the Thorlabs catalog.

A. Background

With the desire for an increase in computational speed, engineers have turned their attention to the use of optical fibers for the production of optical circuits. These optical circuits rely on single mode fibers to transmit information with as little loss as possible, for this reason light needs to be coupled to the fiber as efficiently as possible [6]. Optical circuits aren't the only application for coupling into a single mode fiber, really anytime that a signal is meant to be transmitted down a fiber the light needs to be coupled.

B. Methods

There are a handful of ways to go about coupling light to an optical fiber. One method that has been

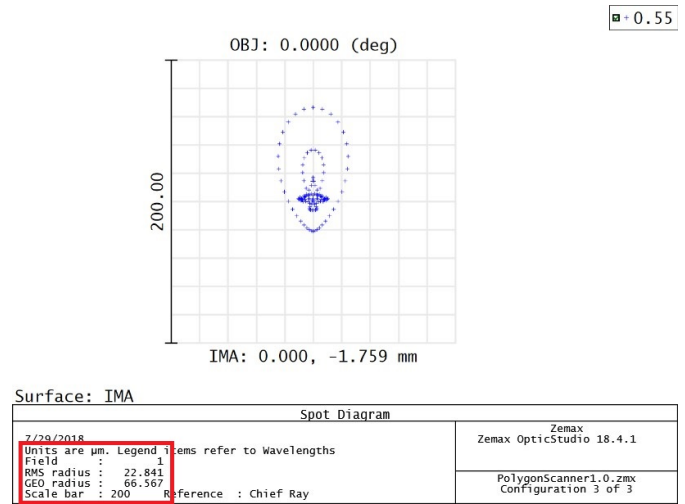


Fig. 7. Maximum angle spot size at $\theta = 5^\circ$. There is a decent amount of Coma through the lens, but most of the intensity is confined to the center of the beam.

suggested is to make a non-sequential component which consists of a pair of cylinders that have different indexes of refraction and focusing light into the core of that component.

A quicker method for coupling an optical fiber involves letting the image plane represent the core of the fiber by giving it some material properties and focusing the light down [7]. There are two methods for analyzing the coupling efficiency through the fiber, one is with the "Physical Optics" function in OpticStudio and the other is with the "Single Mode Coupling" feature. For the purpose of simplicity the "Single Mode Coupling" method was picked.

A 3mm entrance pupil was made to propagate a HeNe source with Gaussian Apodization incident onto a mounted AL1225M-A Plano-Convex Aspheric lens. This lens was chosen due to its low spherical aberration which retains the shape of the input Gaussian beam. The lens has a familiar N-BK7 substrate, optic diameter of 12.5mm , is designed for $350\text{nm} \leq \lambda \leq 700\text{nm}$, and costs $\$208.08$ [8]. The optical fiber which was chosen was 630HP Single Mode optical fiber with a $125\mu\text{m}$ cladding. It is a high performance fiber with a numerical aperture about $N_A = 0.13$, index of refraction $n = 1.4533$, and a cost of $\$5.66$ per meter [9]. So the lens is really quite expensive, but it was relatively easy to find in the lens library of the Zemax lens catalog, and the fiber was easy to find specifications for thanks to Ruvim Kondratyev calling Thorlabs and asking for the index

of refraction for the fiber.

After setting up the environment, the material of the image plane was changed to have an index of refraction $n = 1.4533$ and diameter $3.5\mu\text{m}$ which was identical to the Thorlabs fiber. The AL1225M-A lens was then inserted between the image plane and the stop. In the "Merit Function Editor", an FICL operand was added for a numerical aperture 0.13 [10]. Then Gaussian Quadrature was used with 4 arms and 8 rings to minimize the RMS spot relative to the centroid. Generic boundary conditions were used for glass and air where both minima/edge thicknesses were 0.5mm and the maximum for air was 1m while that for glass was 10mm .

Also, an attempt was made at using the "Physical Optics" function to solve the overlap integral. The beam definition was set for 256 samples in the x and y directions and widths in those two directions of $3.5\mu\text{m}$.

C. Results

After minimization, the merit function reduced to about 0.188 which is decent. The coupling efficiency according to the single mode coupling function can be seen in Fig. 9 to be about -3dB or 50%. The method of using the physical optics function was somewhat confusing, but a plot of the x-cross section of the phase is shown in Fig. 10. The results of the physical optics calculations say that there was a coupling efficiency of about 92%, but that value is somewhat hard to believe in relation to the single mode fiber coupling value. More than likely the values which were entered into the physical optics beam definition and fiber data were incorrect. The X and Y width of the Gaussian beam were entered to be $3.5\mu\text{m}$ to represent the width of the core at the imaging plane and the waist X and Y were entered to be $2\mu\text{m}$ to represent the Mode Field Diameter at 620nm . What may be going on is that the X and Y width are supposed to be for the Gaussian beam before entering the lens, but in that case the coupling efficiency basically goes to zero.

The result that makes the most sense at this point is from the single mode fiber coupling function, which resulted in a layout that is shown in Fig. 8. The beam shows the Gaussian Apodization by increasing the density of rays towards the center of the optical axis and the entire beam obviously comes down to very small waist size at the location of the image screen. One method for coupling optical fibers that would be

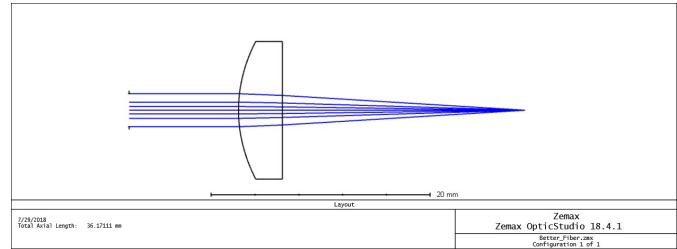


Fig. 8. Layout of lens coupling Gaussian HeNe source into $3.5\mu\text{m}$ optical fiber.

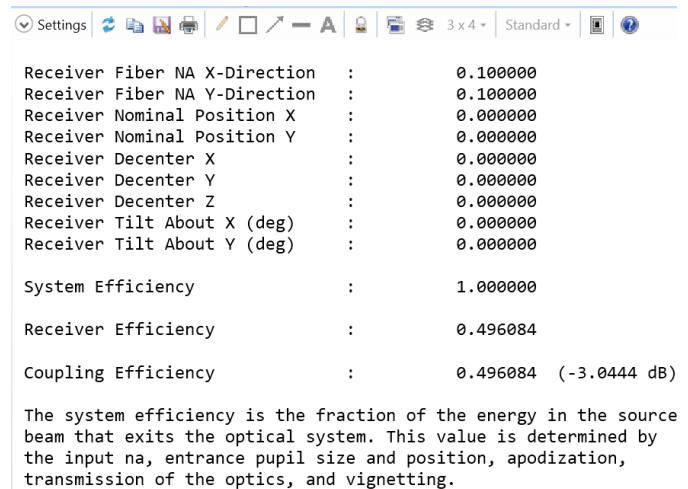


Fig. 9. Coupling Efficiency as seen from Single-Mode Coupling Function.

interesting to test is through ZPL and macros which provide an interesting way to control, model, and analyze this type of system.

3. THE CRYOSTAT

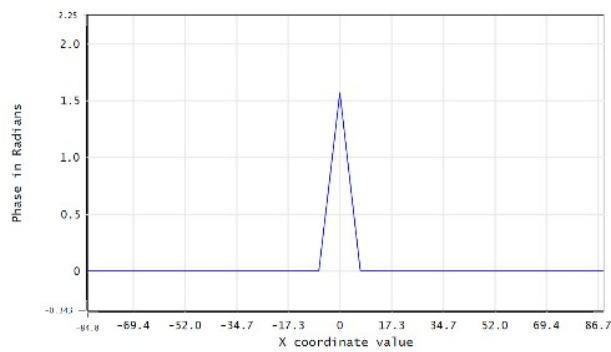
The goal is to minimize the RMS spot size and distortions for an optic that is viewing a sample within a cryostat window. The window is 5mm thick and composed of Quartz.

A. Background

A cryostat is an instrument that can be used to perform spectroscopic measurements on samples at very low temperatures. These devices can get materials to temperatures as low as 4.2K with the assistance of liquid He [11]. Once the sample is sufficiently cold a series of measurements can be taken and an optical device is needed for some of those measurements.

B. Methods

A diagram for a general cryostat was provided, and a closeup with pertinent information is shown in



Phase X-Cross section surface 4	
7/29/2018	
Beam wavelength is 0.63280 um in the media with index 1.46330 at 0.0000 (deg)	
Center: Y = 0.0000E+00	
Center Phase = 1.5704 radians, phase ref to radius 6.0819E+01	
Fiber Efficiency: System 0.920512, Receiver 1.000000, Coupling 0.920512	
X Pilot: Size= 3.8798E+00, Waist= 2.1578E-03, Pos= +0.0819E+01, Rayleigh= 3.3825E-02	

Fig. 10. X-cross section of phase in single mode fiber from Physical Optics calculation of overlap integral.

Fig. 11 where a top-down view of the optical sample holder is boxed and labelled A. A side view of the position of the optical sample holder in the cryostat is shown in the box labelled B. The total width of the sample holder is 82.5mm and the sample will be placed in the very center of the device. This means that the distance from the rear edge of the quartz glass window to the sample is 41.25mm.

A microscope objective design for Zemax was downloaded (US04126377-1) [12] and focused onto an imaging plane. A surface was introduced after the last lens of the microscope objective, it was given a thickness of 5mm and material type *QUARTZ* from the Birefringent library. The thickness from the back of the quartz surface was fixed to be the distance to the sample which was 41.25mm, and the rest of the surfaces of the microscope objectives were set to be variables.

The entrance pupil was set to be 8mm for visible light with two fields, one incident and the other angled 4° from the y-axis. Gaussian Quadrature with 4 rings and 8 arms was used to minimize the RMS spot size with respect to the centroid. The glass boundary values were set to be min 0.5mm, max 10mm, and edge thickness of 0.5mm. The boundary values for the air were set to be min 0.5mm, max 1m, and edge thickness 0.5mm. Axial symmetry was assumed and the merit function for three different configurations after local optimization was about 0.0455 which is very good. The configuration editor was set to thickness operands which were all variable, and resulted

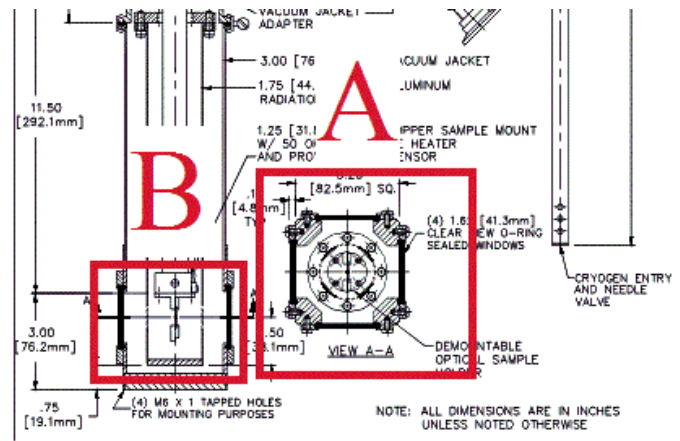


Fig. 11. A top down view of the sample container is labeled A and has a width of 82.5mm. A side view of its position in the cryostat is labeled B.

in two configurations that had optics which were very tightly packed. A handful of different types of glass were used in the design, but weren't modified from the initial types of glass that came from the downloaded microscope objective file.

C. Results

There was one configuration that didn't have optics which were extremely compact, and it seemed to have a reasonable design. The total axial length from the aperture to the sample was about 142mm but the optic itself was 50mm in length (Fig. 12). The final RMS spot size radius that was obtained after performing a local optimization was about 3.84μm for the incident field and 4.06μm for the off center field (Fig. 13). These are relatively small spot sizes, the total diameter for the incident field is about the size of a pixel on a CCD camera.

The total distortion from this optical setup can be seen from the distortion plot in Fig. 14. The distortion plot shows a maximum distortion of about 0.09% at the edge of the lens. The different wavelengths of light are affected by the distortion to varying degrees which can also be observed by the general splitting which appears in the spot diagram in Fig. 13. The distortion is quite small in magnitude and shouldn't drastically impact the results of experiments with this optic.

4. CONCLUSION

This Module began with the design of a Polygon Scanner to sweep a HeNe source through a 10° window. A mirror was placed after an aperture to reflect

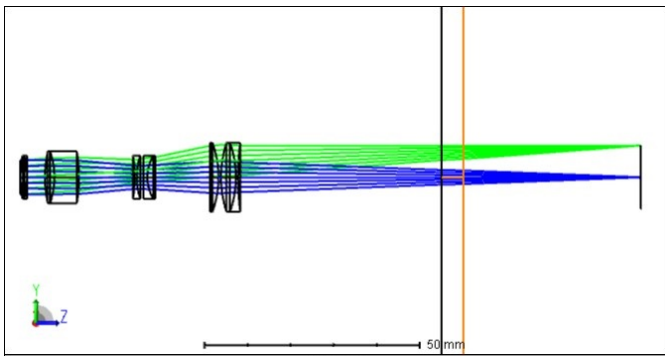


Fig. 12. Cryostat optic configuration. The microscope objective is the set of four lenses to the left, the thin lines in the middle are the quartz window, and the sample is at the imaging plane.

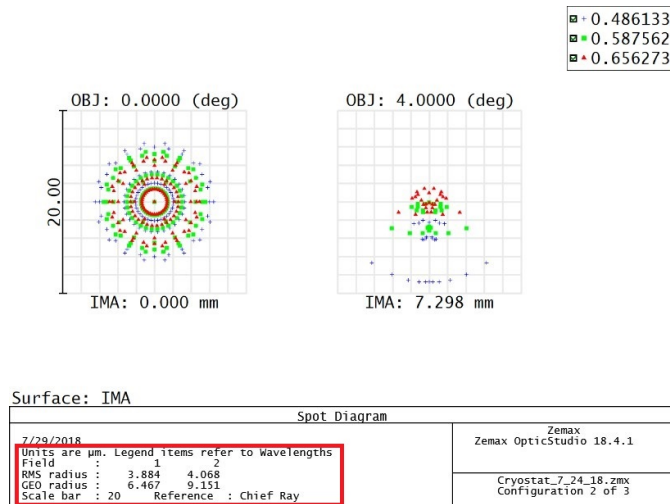


Fig. 13. RMS spot size for visible light through the optic and quartz onto the sample.

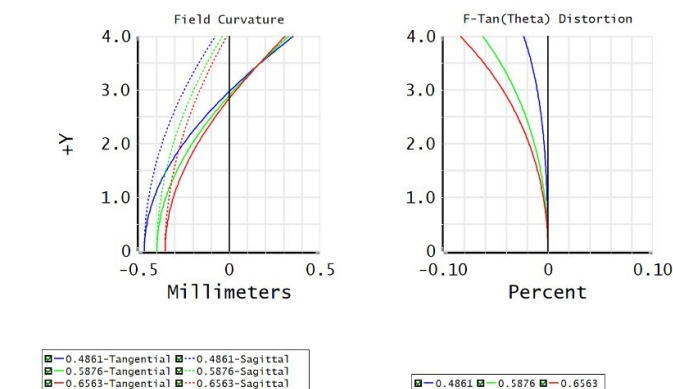


Fig. 14. Ray distortion plot for visible light through optic and quartz.

light toward an imaging plane. The mirror was then given a thickness to correspond to the size of one side of a polygon scanner, and a macro solve was used to decenter the mirror as a function of the angle of rotation. Once the macro solve was operating properly, the scanner was used to optimize a lens in order to minimize the RMS spot size on the imaging screen. The minimal RMS spot size which was found was 19μ for light incident on the lens, and 22μ for light at angles of $\theta = \pm 5^\circ$ from the optical axis. This design was picked because it had the lowest spot sizes that were all very near each other. The polygon scanner would be used for laser etching some material, and having a beam with a beamwidth approximately the same size across all angles is very important despite the size being in the tens of microns range.

The next project involved coupling light into an optical fiber using only products from the Thorlabs catalog. Two methods were attempted for coupling the fiber, one was through the Single Mode Coupling function and the other was through the Physical Optics function. The SMC returned a coupling efficiency of about 50% whereas the PO method returned an efficiency of nearly 100%. More than likely the SMC method was more accurate due to a better understanding of the inputs and calculations that were occurring, in comparison to the PO function where the input parameters were probably incorrectly entered.

The very last portion of the lab involved designing a microscope objective for a cryostat which had 5mm quartz mirrors. The schematic of the sample tray for the cryostat had to be observed in order to understand the geometry of the system and incorporate that into the optical design. A previously designed microscope objective file was downloaded and used as the basis for the optic. A quartz window was placed a known distance away from the imaging screen which was used to represent the location of a sample in the cryostat. Most of the materials were set to be variables and a local optimization was run in order to obtain a decent configuration which had minimal spot size of about $3.84\mu\text{m}$ and distortion at the edge of the field less than 0.1%. The results for the cryostat came out very well. The spot size through the polygon scanner could have been better if proper materials and boundary conditions were chosen. The worst outcome was probably the fiber coupling due to the strange results from the physical optics, although the single mode coupling came out with a reasonable efficiency.

FULL REFERENCES

1. R. De Loor, "Polygon scanner system for ultra short pulsed laser micro-machining applications," *Phys. Procedia* **41**, 544–551 (2013).
2. G. Mincuzzi, L. Gemini, M. Faucon, and R. Kling, "Extending ultra-short pulse laser texturing over large area," *Appl. Surf. Sci.* **386**, 65–71 (2016).
3. Y. Mao, S. Chang, E. Murdock, and C. Flueraru, "Simultaneous dual-wavelength-band common-path swept-source optical coherence tomography with single polygon mirror scanner," *Opt. letters* **36**, 1990–1992 (2011).
4. 612Photonics, *Application of Zemax Programming Language* (2018), online ed.
5. N. Dinyari, "Zemax opticstudio training day 3," (2018).
6. L. Zhu, W. Yang, and C. Chang-Hasnain, "Very high efficiency optical coupler for silicon nanophotonic waveguide and single mode optical fiber," *Opt. express* **25**, 18462–18473 (2017).
7. M. Nicholson and K. Norton, "Single-mode fiber coupling in opticstudio," <http://customers.zemax.com/os/resources/learn/knowledgebase/how-to-model-coupling-between-single-mode-fibers>. Accessed: 2018/7/28.
8. Thorlabs, "Mounted high-precision aspheres: Cnc polished, n-bk7 and s-lah64 substrate," https://www.thorlabs.com/newgrouppage9.cfm?objectgroup_id=8402. Accessed: 2018/7/28.
9. Thorlabs, "Single mode fiber: 600 to 770nm, 630hp," <https://www.thorlabs.com/drawings/78a2c40281e2833e-193DFBB0-EE7F-F23C-FBFC5FF52F856863/630HP-SpecSheet.pdf>. Accessed: 2018/7/28.
10. Z. LLC, "Single mode fiber coupling," <https://www.youtube.com/watch?v=OcC9cPUUJB4>. Accessed: 2018/7/28.
11. P. Naumov, I. Lyubutin, K. Frolov, and E. Demikhov, "A closed-cycle cryostat for optical and mössbauer spectroscopy in the temperature range 4.2–300 k," *Instruments Exp. Tech.* **53**, 770–776 (2010).
12. D. Reiley, "Us04126377-1," <http://www.lens-designs.com/MicroscopeObjectives>. Accessed: 2018/7/23.